# Nocturnal Epileptic Seizures Detection Using Inertial and Muscular Sensors

Osman Salem, Khalid Alsubhi , Ahmed Mehaoua , and Raouf Boutaba , *Fellow, IEEE*

**Abstract**—This paper presents a lightweight approach for the early detection of nocturnal epileptic seizures through analysis of inertial data and muscle contractions. Our approach uses an overlapping sliding window to derive the variance of data acquired by the MPU 9,250 motion tracking device and single channel surface ElectroMyoGram (sEMG). The Exponentially Weighted Moving Average (EWMA) is used to forecast the current value of the data variance. When the Kullback-Leibler divergence between the forecasted and measured variances deviates from past values, a signal is transmitted to the base station to set the current counter in an alarm window. If the filling ratio of the alarm window is greater than a predefined threshold, an alarm is triggered by the base station. The proposed approach is intended to improve the performance of existing detection systems based on data analysis from Accelerometer. The MPU 9,250 is 9-axis motion tracking and used to detect motor seizures, and it contains a 3-axis Accelerometer, Gyroscope, and Magnetometer. The sEMG is used to detect silent seizures without jerky movements. Our experimental results on a real dataset from an epileptic patient show that our proposed approach is able to increase detection accuracy and reduce the low false alarm rate. Comparison with a Probability Density Function (PDF) further demonstrates the detection efficiency of our approach.

**Index Terms**—3D accelerometer, gyroscope, magnetometer, sEMG, epileptic seizures, anomaly detection, EWMA, WBANs

---

## 1 INTRODUCTION

EPILEPSY is a neurological disorder caused by electrical discharges from cortical neurons in the brain, which is susceptible to produce various types of seizure. They are unexpected, unpredictable and unprovoked by an immediate causative factor. More than 65 million persons worldwide suffer from this dysfunction, but in 75 percent of the cases, epileptic seizures can be treated using available therapy (anticonvulsant) or surgery to remove the epileptogenic area [1]. For the rest of the cases (25 percent), the seizures persist despite anti-epileptic drugs and polytherapy, and these drug-resistant patients must live their life with seizures [2].

Patients with epilepsy are usually isolated during the night and vulnerable to several physical injuries or asphyxia due to a blocked airway after swallowing their tongues. They need assistance in short delay during/after the onset of seizures, where falls, fractures and Sudden Unexpected Death in EPilepsy (SUDEP) are frequent. Seizures are particularly risky during the night when patients are isolated and cannot call for help.

The nocturnal seizures may pass unnoticed by the patient's family members and may cause several medical complications or death, and there exists a need to develop a real-time seizure detection system which is able to raise the alarm for family or people in the vicinity when a seizure is detected. Providing assistance may reduce the mortality and prevent further complications (fractures, head-banging, etc.).

The electroencephalogram (EEG) is the dominant method used for the monitoring and detection of epileptic seizures, which usually create abnormalities in the measured EEG signal, and several approaches have been proposed to detect epileptic seizures from EEG signals [3], [4]. The signature of epileptic seizures in an EEG is polymorphic waveforms of variable amplitude and frequency over variable duration. However, existing devices for pervasive acquisition of the EEG signal (helmet, scalp sensors, etc.) are cumbersome, and both uncomfortable to wear in bed and to keep on during sleep.

As epileptic seizure with motor symptoms and uncontrolled jerky movements is the most frequent type (95 percent), and several detection systems based on video processing [5] or motion data analysis from 3-axis accelerometers (ACM) integrated in wristbands (or anklebands [6]) are available in the market. The video processing technique requires a camera and markers on the patient, and when the markers are outside the camera's field of view, the seizure movements are difficult to detect.

Motion analysis techniques using 3D ACM data seeks to distinguish normal nocturnal movements from jerky movements produced by seizures. This practical solution is able to quickly detect nocturnal epileptic seizures with motor manifestations, and raises an alarm for people in the vicinity to limit the seizure's consequences.

We investigated the optimal position for 3D ACM in [7], where we placed three 3D ACMs on the chest, ankle and wrist of a monitored patient. We found that induced

- O. Salem and A. Mehaoua are with the LIPADE Laboratory, University of Paris Descartes, Paris 75270, France.
  E-mail: osman.salem@mi.parisdescartes.fr, ahmed.mehaoua@parisdescartes.fr.
- K. Alsubhi is with the Faculty of Computing and Information Technology, King Abdulaziz University, Jeddah 21589, Saudi Arabia.
  E-mail: kalsubhi@kau.edu.sa.
- R. Boutaba is with the David R. Cheriton School of Computer Science, University of Waterloo, ON N2L 3G1, Canada. E-mail: rboutaba@cs.uwaterloo.ca.

variations by seizures in inertial data are more relevant from the limbs, especially from the ACM on the wrist, where the variations are more visible and easy to detect than data from the ACM placed on the chest. Also, it was found that leg movements were also not involved in all types of seizures.

Given the constrained resources of the wristband devices available in the market, the measured inertial data are transmitted to a Local Processing Unit (LPU—such as a smartphone, tablet, PC, etc.) for motion analysis and seizure detection. As generalized seizures can extend to all or part of the body, they may provoke falls, twitching, sweating, secretions, etc. They can provoke muscle contractions (tonic), or relaxations or alternation between contractions and relaxations (clonic movements), producing shaking when this alternation is fast. When a seizure is detected in the LPU, an alarm can warn family members or healthcare staff. However, data transmission consumes more energy than local data processing, and most of the time, the inertial data are normal and thus their transmission is useless.

Motion analysis techniques have a high False Alarm Rate (FAR), as it is hard to distinguish between daily activities and nocturnal movements from seizures. They are also unable to detect seizures without movements, such as tonic seizures, where the muscles contract without convulsions or motor manifestations. This type of seizure may not be detected through the analysis of inertial data, and requires the analysis of other physiological data. The ElectroMyo-Gram (EMG [8]) involves the detection of electrical signals generated by muscle fibers during contractions. This physiological signal provides valuable information about the state of a patient's muscles, and can be measured using two types of device: electrodes with needle or surface electrodes.

The needle in the invasive method must be in contact with the muscle fiber to measure the produced signal. However, this method monitors the signal emitted by a single fiber and may damage skin and muscle tissues. Their usage is reserved for in-hospital or in-clinic doctors or specialized nurses, and is not adequate for pervasive monitoring.

The acquisition of sEMG signal is based on the use of round patches called surface electrodes, which are fixed on the skin next to the target muscle to enable sEMG [8], [9]. The electrodes measure the signal emitted by a set of muscle fibers and can be easily affixed by any user without the help of healthcare professionals. sEMG has been used for the analysis of movements, muscle strength, fatigue measurements, command of fingers in prosthetic hands of amputee, Human Computer Interface (HCI), speed control of electric wheelchairs, etc.

The most common epileptic seizures are classified in [9] into 4 types: Tonic-Clonic, Atonic, Versive and Myoclonic. The Tonic phase and Versive type induce muscle contractions without convulsions, while the Clonic phase and the Myoclonic type induce jerky movements with muscle contractions. Therefore, one should not expect a strong correlation between sEMG and inertial data in a tonic phase seizure, where muscles contract without notable changes in inertial data. In an Atonic seizure, the patient suddenly loses muscle control, causing them to fall if standing.

Recent detection systems have begun to take into consideration many physiological parameters before raising an alarm through the analysis of Heart Rate (HR), 3D ACM, 3D Gyroscope (GYR), skin temperature, skin conductance, etc. These multivariate systems allow increases in detection accuracy and reductions in FAR.

In this paper, we use inertial and muscular signals to detect the three types of epileptic seizures. The use of sEMG improves the detection accuracy of off-the-shelf wristbands, which are based on the analysis of inertial data. Our proposed monitoring system is able to distinguish normal nocturnal movements from epileptic seizures, and raise an alarm for family members when a seizure is detected. The inertial data from ACMs, GYRs and Magnetometers (MAGs) are used to identify jerky movements in the convulsion phase, and the sEMG is used to detect muscular contractions in the tonic phase.

Instead of applying a change point detection algorithm directly in the data, we look for change detection in the variance of the data, and an overlapping sliding window is used to derive the variance and absorb the variations induced by normal nocturnal movements. The purpose of this proposed approach is to provide online analysis and in-network detection of underlying seizures, intended to work on embedded devices with low processing power. This approach is based on the analysis of two time series: 1 channel sEMG and 1 derived inertial signal. As convulsions induce changes in some of the 9 inertial signals (3 ACM, 3 GYR and 3 MAG), we derive one inertial signal (denoted by $I_t$) that reflects changes in any of the signals by considering the maximum value of variance from whole measured inertial data. In fact, $I_t$ is derived from inertial data ($I_t = f(ACM, GYR, MAG)$) at specific time instants $t$.

The proposed approach involves two steps: forecasting the current variances for sEMG and $I_t$ using EWMA, and analyzing the Kullback-Leibler Divergence (KLD) between the measured and forecasted values. If the KLD deviates, we set the associated time slot in the sliding window, which is used to absorb temporal fluctuations by checking the filling ratio. We built a prototype using an Arduino microcontroller, with e-Health Sensors Shield to acquire the sEMG, and the Inertial Measurement Unit (IMU) MPU 9,250 to acquire 9 Degrees Of Freedom (DOF). To evaluate the effectiveness of the proposed approach, we conducted several experiments after implementing our algorithm in the Arduino. We also used the Shimmer EMG sensor with 10 DOF to acquire only the data from epileptic children in the "rare epilepsies" department at the Necker-Enfants Malades Hospital in Paris, France. Our experimental results show that the proposed system is able to achieve high detection accuracy with low delay and a low false alarm rate.

The rest of this paper is organized as follows. Section 2 reviews relevant related work and different existing approaches for epileptic seizure detection. Section 3 presents our proposed approach for body motion and sEMG data analysis to detect epileptic seizures. In Section 4, we present our results from the experimental evaluations. Section 5 presents a discussion about the proposed approach and Section 6 concludes the paper.

## 2 RELATED WORK

Several approaches for epileptic seizure detection [10], [11], [12], [13], [14], [15] using Wireless Body Area Networks

(WBANs) have been recently proposed to replace the conventional wired EEG through the use of tiny and lightweight devices with wireless transmission.

Various methods to detect motor manifestations during seizures have been proposed in [16], [17], [18], [19]. Today, many devices and wristbands for epileptic seizure detection are available in the market. When the seizure is detected from the inertial data, the system will trigger an alarm [20], [21]. However, existing detection systems are unable to distinguish seizures from similar movement patterns generated by normal daily life activities (brushing teeth, etc.).

Elmpt et al. in [22] proposed a seizure detection model based on HR change. Massé et al. in [23] use the ElectroCardioGram (ECG) to detect seizures from changes in HR. Similarly, in [24], Fujiwara et al. extracted 8 Heart Rate Variability (HRV) features to detect seizures. However, these approaches are subject to high false alarm rates, since the HR increases with nervous system activity and stress state.

As epilepsy seizure induces salivation, involuntary and uncontrolled movements, seizure detection using ACM signals was proposed and experimented on animals in [25], [26] and on humans in [27]. Wang et al. in [26] proposed a three-state finite state machine to detect seizure activities using 1-axis ACM. Nijsen et al. in [27] used 3D ACM to detect seizures and to distinguish them from daily life activities. They analyzed and compared the detection accuracy of four methods based on ACM data: Short Time Fourier Transform (STFT), Wigner Distribution (WD), Continuous Wavelet Transform (CWT), and MODel based wavelet transform (MOD), and found that the features extracted using CWT and MOD provided better classification accuracy (80 percent).

Karmer et al. in [17] proposed a system for seizure detection based on a 3D ACM mounted in a bracelet for seizure detection. The integrated transmitter sends data to a PC for processing and to raise an alarm upon detection of change. Borujeny et al. in [28] proposed a seizure detection approach based on three 2D ACMs positioned on the right arm, left arm and left thigh, and used ANN and K-Nearest Neighbors (k-NN) to distinguish seizures movements from normal movements.

Cuppens et al. in [5] proposed a system based on ACMs and video analysis using Linear Discriminant Analysis (LDA) for seizure detection, where the combined detection had better accuracy. Dalton et al. in [29] developed a template-matching algorithm based on the signature of seizures, and used Dynamic Time Wrapping (DTW) to measure the distance between the ACM data and the template. Becq et al. in [16] used three 3D ACMs positioned on the wrist and the head to detect seizures using norm entropy, which produces better performance than feature-based classification.

In [30], Cuppens et al. extended their previous work in [31] through the use of 4 ACMs attached to the extremities (wrist and ankle) to detect generalized tonic-clonic seizures. They derived a Probability Density Function (PDF) from normal movements to classify data in epileptic and non-epileptic movements. The training phase requires only normal data to derive the PDF, and seizure-related information or annotated training data are not required.

Becq et al. in [16] use three 3D ACMs positioned on patients' wrists and head. Their system achieved 80 percent sensitivity and 95 percent specificity. However, the

performance of the monitoring system depends highly on the position of the ACM. Cleland et al. in [32] investigated the optimal placement of ACMs for detecting a range of everyday activities. Jallon et al. in [1] proposed an epileptic seizure detection system based on the analysis of data received from 2 3D ACMs using the Hidden Markov Model (HMM). The first ACM is attached to the wrist of the monitored patient and the second is placed on the chest. Becq et al. in [33] analyzed the efficiency of epileptic seizure detection using a 3D ACM without limiting the detection to nocturnal seizures, since the patient may be in motion.

Tzallas et al. in [34] compared classification results using Naïve Bayes (NB), k-NN, Decision Tree (C4.5), Logistic Regression, and ANN. They found that ANN achieves the best performance, and this result was confirmed in [10]. Annotated data are required to build the classification model in a supervised manner. However, the annotation task is costly as it requires skill, time and human interaction to classify data in the training phase.

The sEMG is a biomedical signal resulting from the electrical activity during muscle activation. Larsen et al. in [35] focused on tonic seizures using sEMG and a Random Forest (RF) algorithm to classify data into 2 classes: seizure or non-seizure. Conradsen et al. in [2] proposed a multi-modal approach for seizure detection based on sEMG, 3D ACM and angular velocity. They extracted features from the signal details of Discrete Wavelet Transform (log-sum of details in levels 4, 5, 6 and 7), and used the Support Vector Machine (SVM) to classify the data into two groups: seizure and non-seizure. However, SVM requires the training data to build the classification Model. Conradsen et al. in [36] used zero crossings count, DWT and SVM classifier for the automatic detection of tonic-clonic seizures based on sEMG, ACM and GYR. In its objective, this work is the closest to our work on seizure detection based on inertial and muscular activities. However, we use the magnetometer as an additional input, and we rely on lightweight statistical techniques adequate for sensors with constrained resources to achieve better detection accuracy and lower false alarm rate.

## 3 PROPOSED APPROACH

To ensure the early detection of epileptic seizures, we consider a real nocturnal deployment scenario, where a person in bed wears a wristband containing the MPU 9250 capable of acquiring inertial data in real time and a data acquisition interface for sEMG. Muscle activities and patient movements are acquired in real time by the wristband and processed locally for real time detection. Upon detection of a seizure, an alarm is transmitted to the LPU (smartphone) as shown in Fig. 1. The SHIMMER EMG Module, available in the market, is provided inside a small box with a wrist strap for sEMG data acquisition and 10 DoF (ACM, GYRO, MAG and altimeter) and it is smaller and lighter than our prototype and easy to deploy.

Let $X_{i,j} = \{x_{1,j}, x_{2,j}, \ldots, x_{n,j}\}$ denote the measured values for the $j$th attribute (where $j = 1, \ldots, 10$). We denote by attribute the times series associated with the measurements for each axis of the integrated 3D ACM, 3D GYR, 3D MAG and sEMG (9 inertial and 1 physiological attributes). The window of these measurements ($X_{i,j}$) is used to calculate the variance of each attribute and to forecast its next value. The sensor
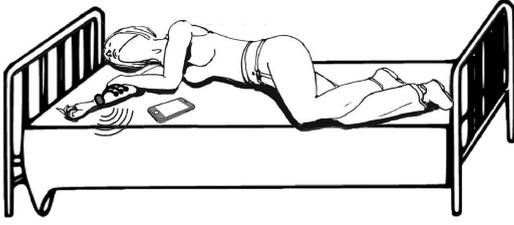
Fig. 1. Bracelet for epileptic seizure detection.



Fig. 2. Predicted and measured variance values.

calculates the variance ($\sigma^2_{i,j}$) of the $n$ measured values for the 10 attributes during the past $T$ time interval. A high variance indicates that the data set has a wide deviation from the mean, while low variance indicates close values.

To reduce the computational complexity and energy consumption in the LPU during seizure detection, we analyzed a feature extracted from multiple signals instead of analyzing the 10 time series obtained from 3D ACM, 3D Gyro, 3D MAG and sEMG. During sleep, the values of raw signals must be close to zero, and Tonic-Clonic (most frequent type of epileptic seizures) provokes convulsions, which induce a large variations in the amplitudes. To detect seizures, we look for changes in these signals (muscular and inertial), where the amplitude characteristics are reflected by the variance of measurements inside sliding window. The variances of the inertial signals and muscular activities are close to zero during sleep (or normal nocturnal movements), and significantly deviate from zero during the seizures. Therefore, we use the variance as a feature to distinguish between normal and seizure data.

To avoid false alarms with normal nocturnal movements, the variance of a sliding window is used to characterize the amplitude and to smooth the short variations. From the variances of acquired inertial signals, the largest deviation value for each period is used to identify change point and to distinguish seizures from normal activities. The maximum value of the 9 calculated inertial (3 axis from each sensor: 3D ACM, 3D GYR and 3D MAG) variances is used to reflect changes and to derive the inertial signal $I_t$ as given in Equation (1). The purpose of this feature extraction is not only to reduce the dimensionality, but to extract useful hidden information in the signals.

Furthermore, the Shewhart limits (derived dynamically from patient profile) prevent the system for raising an alarm for smaller variations. Rarely, normal nocturnal movements and sleep disorders are not often confused with seizures, because they are neither violent nor frequent. However, our system cannot distinguish seizures from parasomnias and frequent movements, which may trigger false alarms due to their similarity with jerky movements. To enhance the reliability of the system, interactions with users are required, where they can push a button to cancel the false alarm and update the patient profile

$$I_t = \max_{j=x,y,z} var\big(ACM_{i,j}, GYR_{i,j}, MAG_{i,j}\big). \tag{1}$$

Accordingly, the sensor derives the variance of the inertial ($I_t$) and muscular signals ($sEMG_t$). We use $V_t$ to denote the matrix $V_t = [I_t, sEMG_t]$. The sensor applies the EWMA to predict the next value ($\hat{\sigma}^2_{t+T,k}$) based on the currently measured and past variances of each signal $I_t$ and $sEMG_t$. The
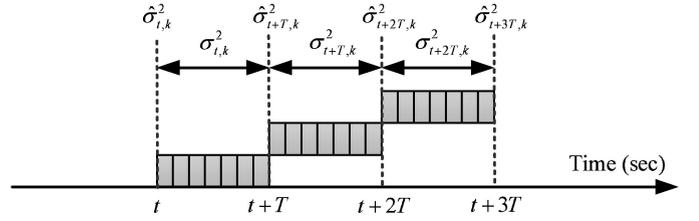
value of $k$ is equal to 1 ($k = 1$) for inertial and $k = 2$ for muscular signal. Afterwards, the detection of divergence (or significant changes) between the predicted and measured values is conducted using KLD and the Shewart control limit.

The EWMA is used for one-step forecasting of $\sigma^2_{t,k}$ as given in the following equation:

$$\hat{\sigma}^2_{t+1,k} = \alpha.(v_{t,k} - \mu_{t,k})^2 + (1 - \alpha).\hat{\sigma}^2_{t,k}. \tag{2}$$

Where $\alpha$ is the weight (or smooth) parameter with a value between 0 and 1. $\hat{\sigma}^2_{t+T,k}$ is the predicted value for the variance of the associated time series ($I_t$ or $sEMG_t$) at the time instant $t + T$. The weighting factor $\alpha$ is a tuning parameter to make the forecasting procedure sensitive to small or gradual drift. It determines the depth of memory and its value ranges from 0 up to 1. The factor $\alpha$ controls the sensitivity of the forecasting procedure and determines the rate at which the current measurement impacts the forecasting procedure. When the value of $\alpha$ is close to 1, the forecasting has small memory and is very sensitive to recent fluctuations in the measured signal, and when its value is close to 0, the procedure gives less weight to recent data and becomes insensitive to normal nocturnal movements. The smoothing factor [37], [38] is recommended to be in the interval 0.05 to 0.25. Our experiments show that alpha = 0.095 absorbs the impact of small disruptions and provides the optimal precision, with high detection rate and lowest false alarms. Therefore we set its value to 0.095 in our experiments.

EWMA is the lightest forecasting procedure in term of computation complexity and storage cost. To predict the current value, it does not need to keep all past measurements, and only uses the previous estimate and the current measurement. EWMA is equivalent to AutoRegressive Integrated Moving Average (ARIMA(0, 1, 1)) with less parameters, and has reduced computational complexity and storage cost. ARIMA model requires a large number of anomaly free observations in training data to derive its parameters. Therefore, robust forecasting using EWMA is preferred, where this simple model generates remarkably accurate forecasts [38]. Similarly, EWMA has the same forecasting precision as KF and IDF after tuning their parameters (as shown later in this paper in Figs. 8c and 8d) with less storage and computation cost. EWMA is appropriate for sensors with constrained resources. We refer to [37] for detailed comparison with ARIMA, KF, GARCH, etc.

Fig. 2 shows the forecasting procedure for one time series, where the EWMA in Equation (2) is used to predict the next value of the variance ($\hat{\sigma}^2_{t+T,k}$) based on past values. In fact, the EWMA will update the forecasted value ($\hat{\sigma}^2_{t+m,k}$) for each new measurement, but we focus only on values at the end of each window ($\hat{\sigma}^2_{t+T,k}$). At the same moment (end
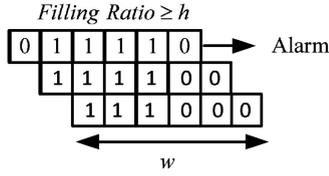
Fig. 3. Window containing alarm counters.

of window with duration $T$), we calculate the variance of measurements in the window ($\sigma^2_{t+T,k}$). Afterwards, the KLD between the measured ($\sigma^2_{t+T,k}$) and predicted ($\hat{\sigma}^2_{t+T,k}$) variances is derived.

The KLD measures the difference between the two probability distributions $P$ and $Q$ as given

$$KLD(P\|Q) = \sum_{k=1}^{2} p_k \log\left(\frac{p_k}{q_k}\right), \tag{3}$$

where $KLD(P\|Q)$ is the mean of the logarithmic difference between probability distributions $P = (p_1, p_2)$ and $Q = (q_1, q_2)$, with $p_k \geq 0$, $q_k \geq 0$, and

$$\sum_{k=1}^{2} p_k = \sum_{k=1}^{2} q_k = 1. \tag{4}$$

The reference probability distribution $P$ is derived from the variances of $I_t$ and $sEMG_t$

$$p_k = \sigma^2_{t,k} / \sum_{k=1}^{2} \sigma^2_{t,k}. \tag{5}$$

The same goes for the derivation of $q_k$ from the estimated variances $\hat{\sigma}^2_{t,k}$ of $I_t$ and $sEMG_t$. KLD has a value equal to or near zero for similar distributions. When the value of $q_k$ deviates from $p_k$, the contribution of the kth term increases and a deviation in the KLD time series for each change is observed. If $p_k = 0$ or $q_k = 0$, the contribution of the kth term is interpreted as zero. The contribution is also zero when both terms are equal to zero ($p_k = 0$ and $q_k = 0$).

We used Shewhart control charts to detect deviations in the KLD. The control chart defines a Center Line (CL) derived from the mean of normal measurements, and when a new measurement is outside the normal range $[LCL, UCL]$ defined by the Lower Control Limit (LCL) and Upper Control Limit (UCL), a change is detected. These limits are computed as 3 standard deviations above and below the CL

$$LCL = CL - 3 \times \frac{\sigma}{\sqrt{n}} \tag{6}$$

$$UCL = CL + 3 \times \frac{\sigma}{\sqrt{n}}. \tag{7}$$

The control charts do not require normally distributed data, and can work with any input distribution. If the value of KLD is inside the range $[LCL, UCL]$, the measured data are more likely generated by hypothesis $H_0$ (or normal hypothesis); otherwise, we reject the normal hypothesis (also denoted by null hypothesis or $H_0$) and assume a change to another hypothesis ($H_1$).

When a significant statistical change is detected in at least one time series (inertial or sEMG), a signal is transmitted to

the LPU to set the associated time slot in the sliding window (as shown in Fig. 3). To achieve a good detection ratio and to reduce false alarms triggered by transient motions and temporal fluctuations, the LPU uses the Filling Ratio (FR) of the sliding window (Fig. 3) before raising a medical alarm. When the FR is greater than predefined threshold $FR \geq h$, an alarm is triggered by the LPU.

Algorithm 1 shows the pseudo code of our proposed approach, where the LPU derives one inertial time series from the 9 received inertial signals. The muscular activities (sEMG) and the derived inertial signals acquired during the past time interval $T$ are used to calculate the variance of each signal ($\sigma^2_{t,k}$) and to predict the next values ($\hat{\sigma}^2_{t+T,k}$). If the KLD between the measured and predicted distributions of the variances is outside the range defined by the Shewart control charts, the associated time slot is set. To reduce false alarms, when the FR of the sliding window is greater than $h$ ($FR \geq h$), an epileptic seizure alarm is raised to call for help.

---

**Algorithm 1.** Pseudo Code for our Proposed Approach

---

1: **function** ONSENSORPROCESSING(none)
2:    **for** ($j = 1 \rightarrow 10$) **do**
3:       $\sigma^2_{i,j} \leftarrow window.variance(X_{i,j})$
4:    **end for**
5:    $I_t = \max\big(variance(ACM_{i,j}, GYR_{i,j}, MAG_{i,j})\big)$
6:    **for** ($k = 1 \rightarrow 2$) **do**
7:       $\hat{\sigma}^2_{t+1,k} = \alpha.(x_{t,k} - \mu_{i,k})^2 + (1 - \alpha).\hat{\sigma}^2_{t,k}$
8:       $p_k = \sigma^2_{t,k} / \sum_{k=1}^{2} \sigma^2_{t,k}$
9:       $q_k = \hat{\sigma}^2_{t,k} / \sum_{k=1}^{2} \hat{\sigma}^2_{t,k}$
10:   **end for**
11:   $KLD_t = \sum_{k=1}^{2} p_k \log\left(\frac{p_k}{q_k}\right)$
12:   **if** ($KLD_t < LCL$ or $KLD_t > UCL$)) **then**
13:      $AlarmWindow_t.set()$
14:   **end if**
15:   **if** ($Window.FR(AlarmWindow) \geq h$) **then**
16:      Raise an epileptic seizure alarm
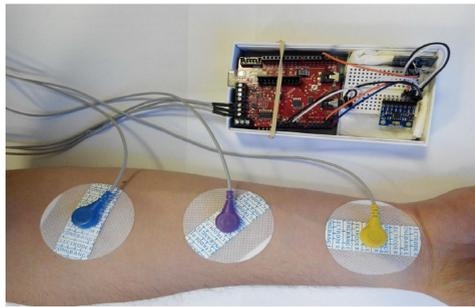17:   **end if**
18: **end function**

---

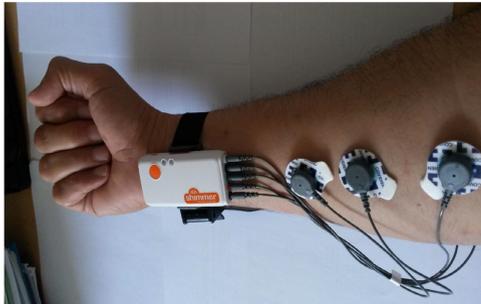# 4 PROTOTYPE IMPLEMENTATION AND EXPERIMENTAL EVALUATIONS

In this section, we present the experimental results of the proposed approach for epileptic seizure detection using real data from epileptic patients and data from simulated seizures. We further evaluate and compare the performance of our proposed approach with that of the Probability Density Function based approach presented in [30]. We also replace the EWMA forecasting procedure with a Kalman Filter (KF) and Implicit Dynamic Feedback (IDF) for further performance comparison.

## 4.1 Prototype Implementation and Evaluation Setup

To evaluate the proposed approach, we built a prototype using an Arduino Uno microcontroller (as shown in Fig. 4a), where we implement our proposed algorithm. We connect the Cooking-Hacks [39] interface to the Arduino to measure the single channel sEMG signal through the use of 3 wired electrodes. We also connect the IMU chip MPU9250 containing the 3D ACM, Gyro, MAG and Radio Frequency

(a) Used prototype



(b) Shimmer EMG

Fig. 4. Real deployment scenario.



Fig. 5. Myo armband and its integrated sEMG sensors.

(RF) transmitter. The validation of the detection system is realized on healthy persons and epileptic patients.

Acquiring the signal sEMG typically requires skin cleaning and pre-gelled electrodes. However, recent technological advances allow us to acquire the sEMG signal without using wet sensors or sticky gels with electrodes, e.g., the electrical sensors used in Myo armband [40], [41] to acquire the sEMG are shown in Fig. 5. Three flat metal pieces are used as 3 electrodes to acquire the micro-voltage signal, and a board circuit for signal amplification (and digital processing) are integrated in each of 8 components (or casinghouse) of the Myo bracelet.

However, the deployment of our prototype in the "epilepsies rares" department at the "Necker-Enfants Malades" Hospital posed some problems. Many children did not feel safe wearing our prototype and removed the cable/electrodes, even when we tried to hide the microcontroller under their pillows. Therefore, we replaced the prototype with one Shimmer3 EMG (shown in Fig. 4b) in our last experiments for data collection. The latter (Shimmer3) contains an integrated altimeter, 9 DoF and two channels sEMG, but we only used one channel sEMG and 9 DoF. The Shimmer deployment was also difficult, but most children ended up accepting it after covering the box with a wristband sponge bob. Obviously, the main reasons that prevented the deployment of our Arduino prototype (shown in Fig. 4a) were its size, weight and shape which were not child-friendly.

The first evaluation test was conducted by 7 healthy volunteers to verify the correctness and reliability of the proposed detection system. All the patients involved in the development of this project were male between 25 and 50 years old. The prototype (inside the box) was attached to the wrist using a rubber band, and a special cream was used to fix the 3 electrodes and prevent their disconnection from the forearm. It is important to note that in some of the experiments, electrodes were involuntarily disconnected by nocturnal movements or sweat. Data collection was performed overnight, and an evaluation test was conducted to verify the functioning of the prototype and to tune its parameters.

Algorithm 1 is evaluated as part of the prototyped monitoring system for epileptic seizure detection. The precision of the prototype is evaluated is terms of false alarms and true detection of epileptic seizures. The monitoring system raises an alarm every time the FR is greater than or equal to the predefined threshold $h$. The quality of the acquired data is evaluated by the detection accuracy of the monitoring system in terms of true detection and false alarm rate.

The comfort of using the prototype was evaluated by the volunteers after the data collection phase. Their experience wearing the prototype was not as comfortable as with the Shimmer, but even the Shimmer prototype still far from being the perfect solution for the real scenario. They proposed to use an armband (similar to the Myo Armband [42]) with a built-in device for acquiring sEMG and inertial signals, instead of wired electrodes with Arduino (or Shimmer) in our prototype.

## 4.2 Results

The second real dataset (containing seizures) is collected using Arduino microcontroller, with the e-health complete kit and the MPU 9250. All monitored children (8 children) wear the developed prototype (wired sEMG electrode and IMU) before going to sleep (after the lunch/dinner) to collect inertial and muscular data for several hours. Only 4 datasets were exploitable from 32 collected datasets over several days in the "epilepsies rares" department at the Necker-Enfants Malades Hospital in Paris, France.

Given the deployment complexity, we conducted third collection phase, but we used the Shimmer3 IMU as prototype instead of Arduino. The sampling frequency was 512 for whole signals. More than 110 motors seizures from different children were collected over one month and used for performance analysis of the proposed detection system. In most cases, we observed one seizure by children through the monitoring day, with mean duration between 10 and 30 seconds. In few extreme cases, the seizure lasts 3 minutes. We concatenate 100 seizures into one file to build a synthetic trace for performance analysis.

Each dataset contains the inertial and muscular measurements for several hours. All patients were taking anti-epileptic drugs to reduce the frequency of seizures and improve their quality of life. In this paper, we only focus on approximately 5-minute periods, including the seizure. The
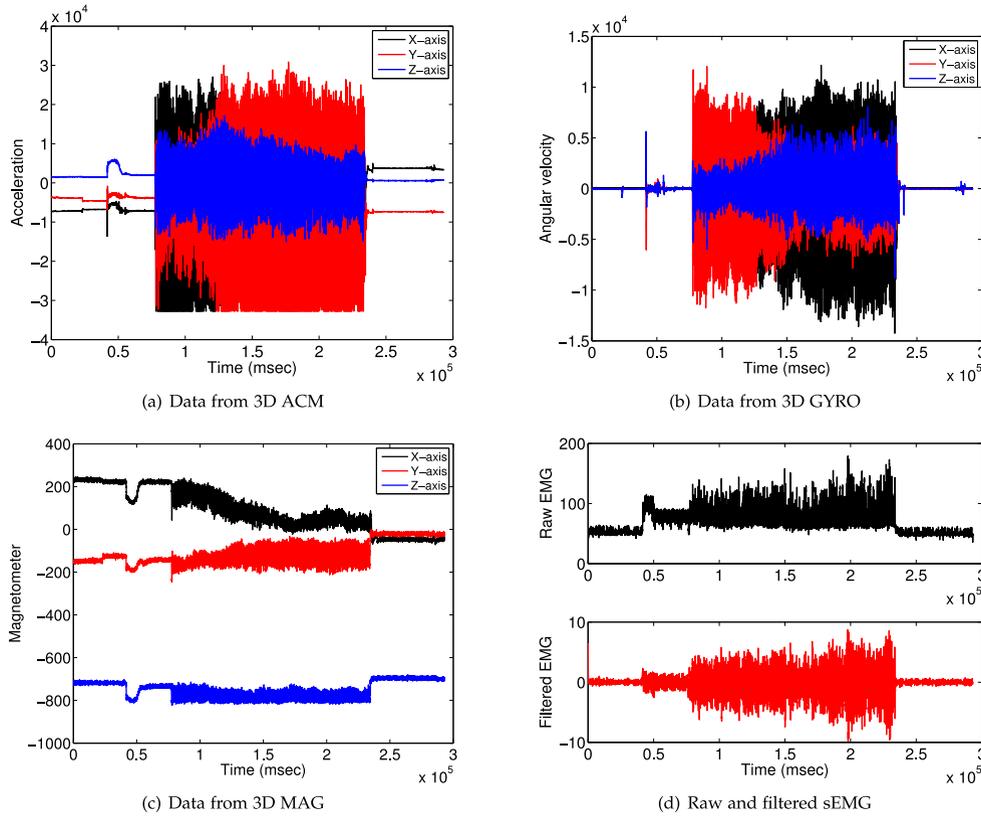
Fig. 6. Inertial and muscular data.

raw collected data from the monitored patients during tonic-clonic seizures by the IMU (3D ACM, GYR, MAG) and muscular electrodes (sEMG) are presented in Figs. 6a, 6b, 6c, and 6d respectively. The filtered sEMG is also shown at the bottom of Fig. 6d.

The raw EMG signal requires preprocessing to remove noise and movement artifacts. A band-pass filter with cutoff frequency of $[20 - 400]$ Hz, was used to remove frequencies associated with noise and artifact, and to preserve the desired information related to muscle activity. We used a low pass filter with cut-off frequency of 20 Hz to remove the motion artifact, and a high pass filter with cut-off frequency of 400 Hz to remove noise outside the band of interest. These filters are provided by the shimmer API for software development [43], [44].

We can visually identify in the inertial data (Figs. 6a, 6b, and 6c) a small variation during the tonic phase, and large variations during the clonic seizure phase are visible on all axes (X, Y and Z) around the interval $[80, 220] \times 10^3$ msec. Small deviations from zero around the time instant $0.5 \times 10^5$ msec are induced by the tonic phase, which mostly produces muscle contractions and precedes the clonic phase.

A visual inspection of the filtered sEMG signal in Fig. 6d shows the underlying variations generated during the tonic and clonic phases, and we can notice correlations between the inertial and muscular activities in both phases. However, the sEMG signal detects the tonic phase faster than the inertial signal.

A sliding window containing acquired data in 1 sec, with an overlapping ratio of 50 percent, is used to calculate the variance of inertial and muscular signals on the sensor. The variances of the signals acquired from the 3D ACM, GYR, MAG and sEMG are shown in Figs. 7a, 7b, 7c and 7d respectively. The local processing allows reducing energy consumption by the data transmission and prolongs the life of the monitoring system.

The microcontroller derives one inertial signal $I_t$ from the 9 signals presented in Figs. 7a, 7b and 7c by considering the maximum value to reflect the variations in any signal. To predict the current value of the variance, we tested 3 forecasting procedures: EWMA, KF and IDF. The measured ($\sigma^2_{t,k}$) and forecasted ($\hat{\sigma}^2_{t,k}$) values of the data variance from the inertial and muscular signals are shown in Figs. 8a and 8b. However, these forecasting procedures achieve similar performance by changing the values of their parameters, as shown in Figs. 8c and 8d. In fact, we cannot distinguish between the overlapping curves as they predict the same values. Regardless, we choose EWMA in our implementation for its simplicity.

From the variance of raw inertial data presented in Figs. 6a, 6b and 6c, the signal $I_t$ (maximum variance) is derived and presented in Fig. 8a with the forecasted signals using different algorithms. The difference between the forecasted and measured values ($\zeta_{t,k}$) of the variance of the inertial activities (Equation (8)) is shown in Fig. 9a. The same goes for raw muscular activities presented in Fig. 6d. The derived filtered sEMG is also shown on the bottom of Fig. 6d, and has been used to calculate the variance of measurements in a sliding window (shown in Fig. 7d) and the forecasted variance at the end of each window (shown in Fig. 8b), as well as the difference between the measured and forecasted values (shown in Fig. 9b)
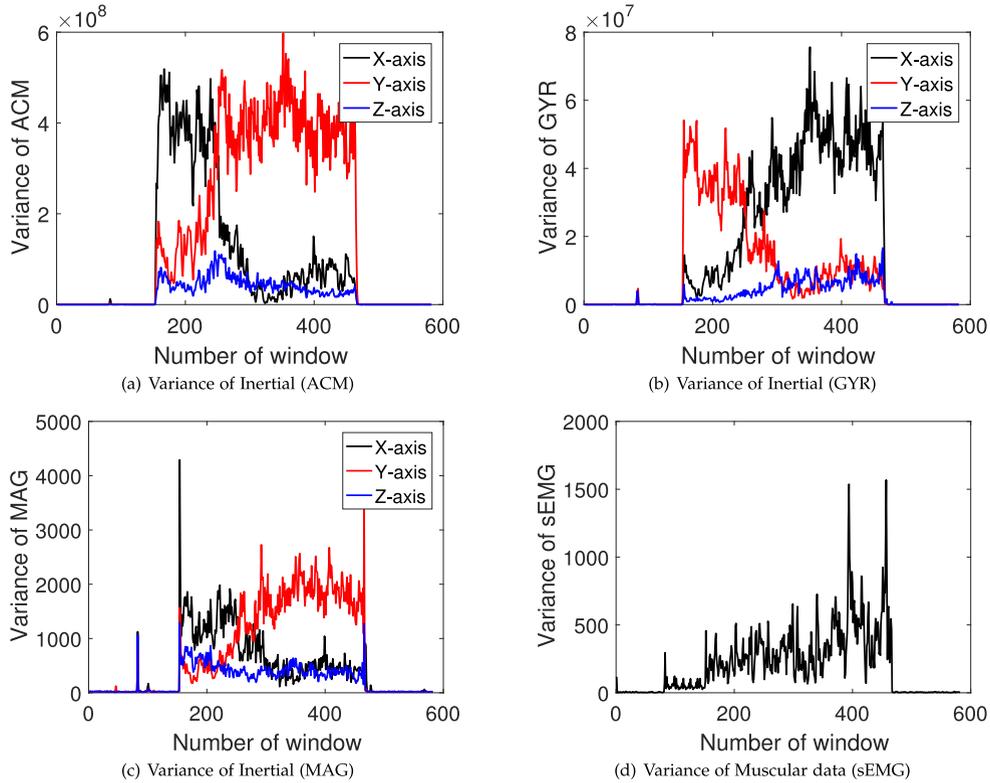
(a) Variance of Inertial (ACM)

(b) Variance of Inertial (GYR)

(c) Variance of Inertial (MAG)

(d) Variance of Muscular data (sEMG)

Fig. 7. Variance of measured data.

$$\zeta_{t,k} = \hat{\sigma}^2_{t,k} - \sigma^2_{t,k}. \qquad (8)$$

Where $t$ denotes the time reference and $\zeta_{t,k}$ is calculated only at time instants $t = k \times T$. The possible values of $k$ are 1 and 2, where $k = 1$ for inertial signal and $k = 2$ for sEMG.

During tonic-clonic seizures, patients usually start with muscle contractions followed by involuntary and uncontrolled jerky movements in the clonic phase, thus inducing a deviation between the measured and predicted instances of $V_t$. The KLD between the measured and forecasted variances in $V_t$ is shown in Fig. 9c, and fluctuates during the changes generated by a tonic-clonic seizure. To detect changes in the KLD, we used control charts for online change detection, where a signal is transmitted to the LPU if the value of KLD exceeds one of the control limits (UCL or LCL), as shown in Fig. 9d.

When the FR of the sliding windows (shown in Fig. 3) is greater than a percentage $p\%$ for a window size $w$ time slots, an alarm is triggered by the LPU. A large value of $w$ induces large detection delay and makes the system inefficient in the detection of seizures of short duration. Therefore, the value of $p$ must be chosen as a tradeoff between false alarms and detection accuracy. A large value of $p$ will decrease the false alarms and the detection accuracy, and vice versa. The optimal values of $p$ was determined empirically and set to 10 percent in our experiment for a window size $w = 30$.

The alarm was triggered for seizures in Figs. 6a, 6b, 6c and 6d at time instant 45,000 msec. However, it is important to note that there is no significant difference in the detection accuracy when considering a FR with a value greater than or equal to 10 percent. In contrast, a low FR value significantly increases the false alarm rate. Therefore, the value of FR is a trade-off between false alarms and detection accuracy.

The detection delay of seizures by our approach is 3 sec, which is very reasonable when compared to existing approaches and directly related to the threshold $h$. However, the detection delay is a tradeoff between false alarms and true detection. Its value follows $h$, where a small value of $h$ reduces the delay and increases the rate of false alarms, and a large value of $h$ increases the delay and reduces the false alarms.

### 4.3   Performance Analysis

We start the performance analysis experiments by analyzing the impact of parameter $\alpha$ on the predicted values of the variances. We present the results for the inertial data only. Fig. 10 shows the impact of the weighting factor on the prediction process of variance. By choosing a value of $\alpha$ near to 1, the predicted time series becomes more sensitive to the new value of the measured variance and its transient fluctuations. We use $\alpha = 0.095$ for a regular data smoothing and to minimize the impact of fluctuations by giving more weight to past values. Furthermore, this small value allows distinguishing convulsions from normal nocturnal movements.

To evaluate the performance of our approach, we use a synthetic data set containing 100 seizures at different time instants. This dataset is built by concatenating several real data collected during seizures collected using Shimmer3 unit, and mostly contains one seizure. The Shimmer3 unit acquires motion (IMU) and biophysical (sEMG, GSR, Respiration, etc.) with a sampling rate of 512 Hz for ACM, GYR, MAG and sEMG. We apply our algorithm on the resulting synthetic dataset to study the impact of the threshold $h$ on the detection accuracy. We used the Receiver Operating Characteristic (ROC) curve to show the impact of $h$ on the True Positive Rate (TPR) given in Equation (9) and the False

(a) Variance of Inertial

(b) Variance of Muscular

(c) Variance of Inertial data
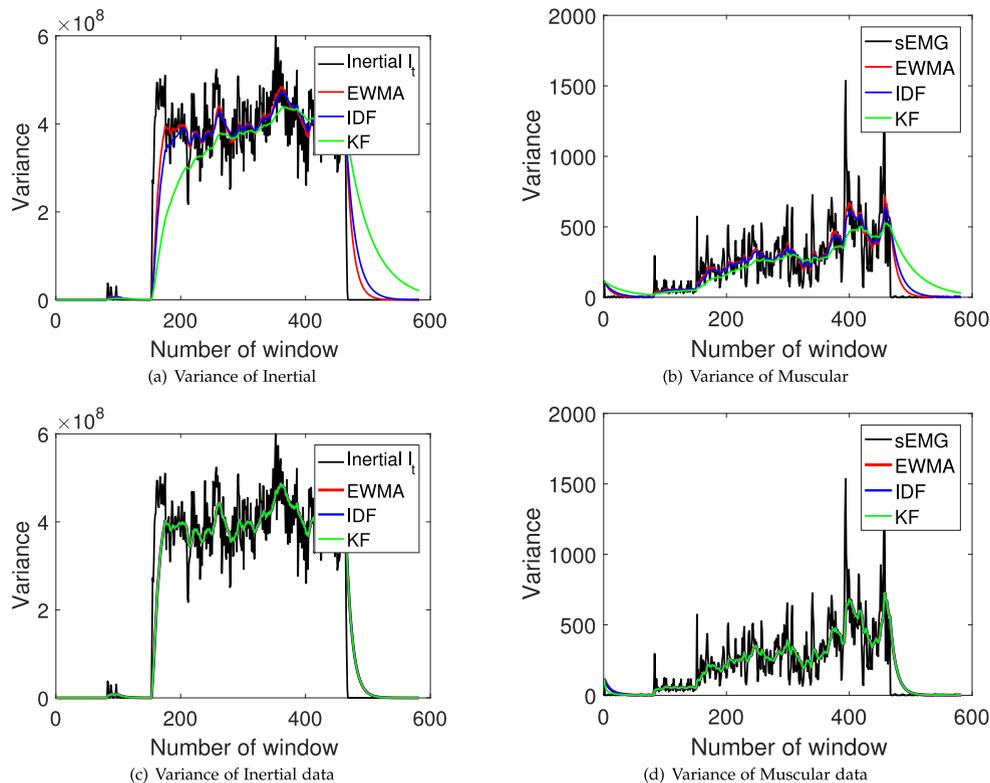
(d) Variance of Muscular data

Fig. 8. Measured and forecasted variances.

Alarm Rate given in Equation (10)

$$TPR = \frac{TP}{TP + FN} \times 100\%, \quad (9)$$

where $TP$ is the number of true positives, and $FN$ is the number of false negatives. FAR is defined as the ratio of incorrectly detected seizures

$$FAR = \frac{FP}{FP + TN} \times 100\%, \quad (10)$$

where $FP$ is the number of false positives and $TN$ is the number of true negatives. A good detection mechanism should achieve a high detection ratio with a low FAR.

To demonstrate the effectiveness of our approach, we conduct comparisons with Multi-model Intelligent Seizure Acquisition (MISA) system proposed in [9] and the Probability Density Function in [30], [45] to detect seizures. The MISA uses multi-modal (sEMG, ACM and GYRO) to propose an automatic method for the detection of seizures with motor manifestations. MISA uses discrete wavelet decomposition (Daubechies) to derive approximation ($A_1$) and Detail ($D_1$) of level 1. These signals are the result of low and high pass filters respectively. From each approximation $A_i$ in level $i$, the same filtering procedure is applied to split the signal into $A_{i+1}$ and $D_{i+1}$. Each channel from ACM and GYRO is divided into 6 levels, and sEMG into 7 levels.

The sampling frequencies for their input sEMG was 1,024 and 120 Hz for ACM/GYRO. Conradsen et al. [9] apply wavelet decomposition on overlapping sliding window of 1 second, i.e., each window contains 120 samples for inertial and 1,024 samples for sEMG, with an overlap of 50 percent between 2 consecutive windows. To reduce the number of input signals obtained for seizure detection, they derive a

feature vector $x$ carrying the amount of energy contained in the frequency range for seizure events. For the ACM/GYRO signals, the frequencies extracted are 0.94-7.5 Hz and for the sEMG signals they are 4-64 Hz. These frequencies were identified through visual inspection of the signals' spectrum. The optimal Support Vector Machine is used to classify the vector $x$ into two classes: seizures and normal. The class seizures contains whole epileptic seizures and the normal class contains normal nocturnal data without seizures. From 152 channels, 14 sEMG channels and 138 channels of 3D ACM and 3D GYR (23 × 3 ACM and 23 × 3 GYR), MISA achieves a good performance with TPR 100 percent, FAR of 5 percent and latency of 1 second.

To compare the performance of MISA with that of our approach, we use wavelet decomposition with 6 layers for sEMG and 5 layers for ACM/GYRO (3, 4, 5, 6 for sEMG and 3, 4, 5 for ACM/GYRO) to calculate the log-sum from detail signals and to derive the feature vector $x$ [9], as the sampling frequency of our combined data for this experiment is 512 Hz. A training data with 10 seizures is used to derive the SVM hyperplane (separator line between 2 classes) used to classify the feature vector $x$. To reduce the false alarms with the small number of channels in our experiment (10 channels instead of 152 channels used in their experiment), skewed (unbalanced) classes and incomplete training data with whole possible normal movements, we added the use of FR of the alarm sliding window as in our approach.

Fig. 11 shows a comparison between the ROC of the proposed approach, the MISA and the ROC of the PDF method for the same dataset. The TPR of our proposed approach reaches 100 percent for a FAR of 6 percent, and the TPR of the PDF method also reaches 100 percent for a FAR of 9 percent, and the TPR of the MISA also reaches 100 percent

(a) Error on inertial

(b) Error on muscular

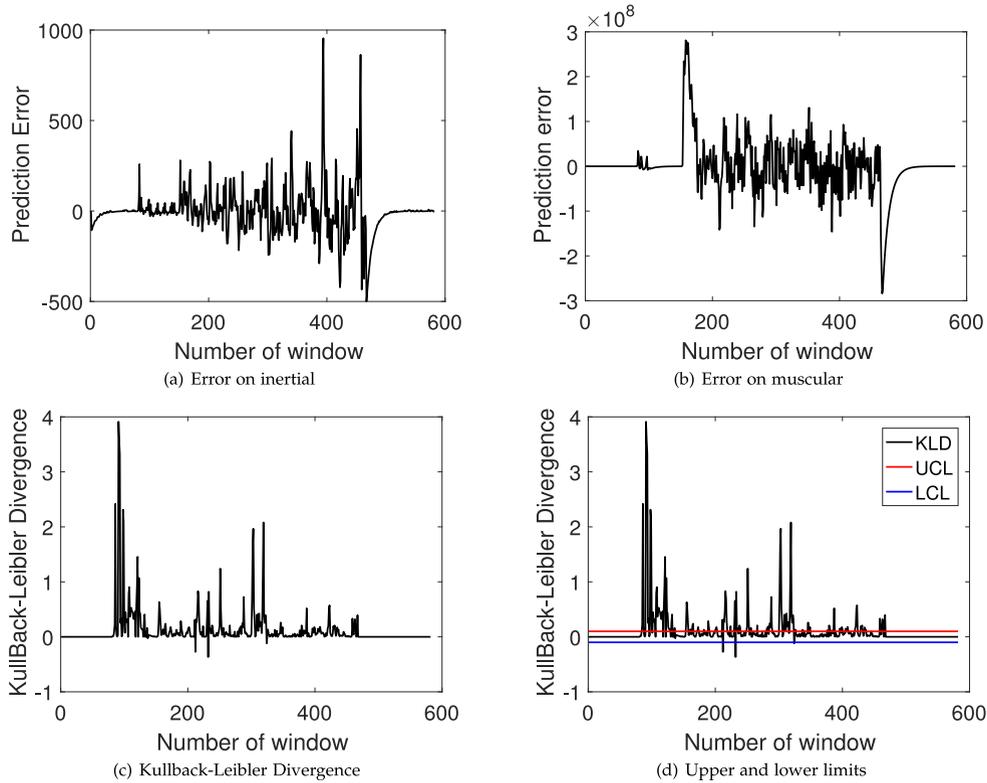(c) Kullback-Leibler Divergence

(d) Upper and lower limits

Fig. 9. Change detection.

with a FAR of 13 percent. For 95 percent of DR, our approach triggers 4 percent of FAR while PDF triggers 7 percent. The ROC curve of the proposed system outperforms the ROC of PDF and the MISA methods by reducing the number of false alarms. It is important to note that our implementation of PDF is based on KDE, and that the same input dataset is used for the 3 methods.

When applying MISA, the computation complexity for classification in SVM used in MISA is $\mathcal{O}(1)$. In fact, the classification of new record is achieved by comparing the derived feature with the hyperplane. However, the required complexity to derive the classifier from training data is $\mathcal{O}(n^3)$, where $n$ is the number of records in training data. Therefore, the required computational complexity to derive (and to update) the classification model may quickly deplete the energy of the sensor. Furthermore, the required labeled training data to build the classifier is hard to derive and adds

significant load, where 2 seizures from the same patient do not exhibit the same contraction strength and convulsion pattern.

On the other hand, the computation complexity to derive the PDF from the $n$ measurements is $\mathcal{O}(n^2)$, which makes it prohibitively expensive for sensors with constrained resources and for large amounts of data. The complexity to predict and to derive the variance is linear $\mathcal{O}(n)$, where $n$ is the number of elements in the sliding window. Therefore, our proposed method has a computational complexity of $\mathcal{O}(n)$, which is more adequate than SVM and PDF in deployment environments with constrained resources. Our approach is lighter than MISA in terms of computation complexity, memory usage and number of required sensors.

## 5 DISCUSSION

### 5.1 Impact of Additional Biosignals

The reliability of existing seizures detection systems prevent their adoption and wide deployment, especially when considering their high rate of false alarms and inability to detect seizures without jerky movements. The $FAR$ and the detection of non-convulsive seizures in our proposed detection system can be enhanced by considering additional biosignals. Several physiological parameters may change during seizures, such as Heart Rate, respiration (RESP) rate, skin conductivity or Galvanic Skin Response (GSR), body temperature, etc. The HR, RESP, GSR, skin temperature, can be easily acquired by the armband, where many existing activity trackers are able to acquire these parameters in non-invasive manner. On the other hand, patient comfort must be taken into account, and his body must not be overloaded with biosensors. An optimal set of physiological parameters
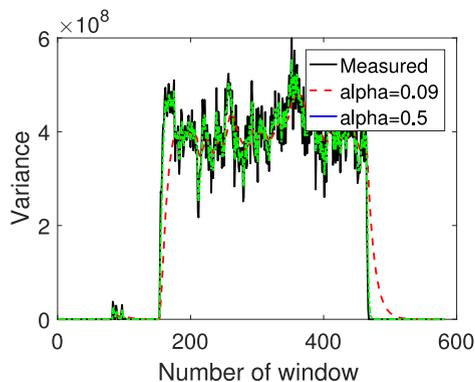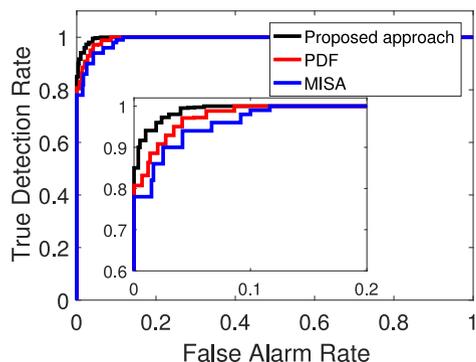


Fig. 10. Impact of weighting factor ($\alpha$).

Fig. 11. ROC.

must be identified to achieve both accuracy and comfort in our future work.

## 5.2 Impact of Design and Acceptance

To the best of our knowledge for existing seizures detection devices in the market, the acceptance by children has not been addressed. Children refuse to carry the device and start screaming. We tried to make it appear as an attractive bracelet (by including popular characters such as sponge bob, Frozen Queen, etc.). This should be considered at the conception phase to provide an attractive armband that appears as a game for children with lullaby. In the other hand, our prototype for seizure detection uses only an armband to acquire inertial signals and muscle contractions. The use of armband with non-invasive recording (sEMG) was more accepted than EEG-based systems (headsets) with motion sensors, and more accurate, with lower false alarm rate when comparing with 5 channels EEG Emotiv [46], [47] headsets with integrated inertial sensor (9 DoF) to detect head movements. It is more practical to sleep (and to keep during sleep) with armband than headsets.

The Emotiv was used to capture the EEG data and a software was used to process the acquired EEG signals by the headset. The use of 5 channels in EEG, instead of widely used 32-channels in hospital, reduces the detection accuracy, where the electrodes are unable to cover whole area in the brain, especially when fired neurons are far from electrodes. The electrodes must be placed on the lesion (location of epilepsy) for accurate detection. Therefore, the deviations generated by some seizures was not detectable as we do not have access to the relevant channels.

Furthermore, it is hard to keep the electrodes in contact with daily life activities. As the children were observed by nurses, the recorded EEG signals contain artifacts and several additional variations identified as seizures by the neurologist and by assistive automatic detection tools. This can be explained by unrestricted movements (eye blinking, turning, etc.) and the associated artifacts. The false alarms are identified from the notes of nurses written during daily observation. The detection rate for one day on all monitored patients was 76 percent with a FAR of 14 percent.

Different EEG based detection systems are available today and have different accuracies. Conradsen et al. in [48] compare seizure detection approaches based on sEMG with existing approaches based on EEG. They found the detection rate for EEG based systems varies between 70-100 percent with a 0.5-72 false alarms per day, where the accurate system uses more than 60 electrodes.

## 5.3 Human Activity Recognition

Our proposed system is intended for nocturnal detection and requires a combination with additional mechanisms for the detection during daily activities. We are working on human activity recognition and behavior tagging, by allowing the user to create a model for each activity (walking, running, cycling, driving, brushing teeth, etc.). A training period of five minutes is required for each activity, and is requested from user to derive the statistical parameters of the user custom activity. During test phase, an activity with statistical parameters that heavily deviate from pre-established profiles of recognized activities is classified as seizure. Users must also have the ability to interact with the monitoring system, where he can push a button to cancel ongoing false alarm for seizure. The detection system can derive the parameters of current pattern and store them to prevent such false alarms in the future and improve the accuracy of the detection system.

We are working on enhancing the detection system by taking into account the sex, age and weight of the patients. We analyzed the mean number of minutes that children spent in moderate or vigorous activity to distinguish with seizures and to enhance the accuracy of our detection system. We conducted studies for boys and girls separately considering age and weight to determine the differences across childhood. There were no significant differences for vigorous activity between girls and boys in all groups. Our analysis showed that children (girls and boys) in each group spent very little time in sustained activity, only overweight children spent less time in vigorous activity. Furthermore, during class time, children (6-17 year old) have reduced activity and such context-aware information can be exploited to enhance the accuracy of the detection system.

## 6 CONCLUSION

In this paper, we have proposed a lightweight and efficient approach for the automatic detection of epileptic seizures. Tonic-clonic seizures are the most common type of seizure. They have motor manifestations, muscle contractions, or both. Jerky movements can be detected through real-time data analysis from ACM, GYRO and MAG, and muscle contractions can be detected by analyzing the data from sEMG. The muscular contractions followed by abnormal jerky movements are used by our approach to detect nocturnal seizures and to raise an alarm. The combination of inertial and muscular signals increases the detection accuracy and reduces the rate of false alarms. Furthermore, it allows the detection of different types of epileptic seizures.

The proposed approach is based on the analysis of inertial and muscular data, and is aimed at enhancing the detection accuracy of existing devices while reducing energy consumption by eliminating the transmission of normal data to the LPU. The early detection of seizures is based on change point detection in the Kullback-Leibler divergence between measured and forecasted variances. A signal is transmitted to the LPU upon detection of a change, and sets an associated counter in a sliding alarm window. The LPU

uses the filling ratio of the alarm window to make a final decision and raise an alarm to family members or healthcare professionals.

We used simple and computationally efficient methods capable to absorb normal nocturnal movements and highlight convulsion seizures. The advantages of our approach are the independence from the labeled training data required to build a classification model for machine learning, and the local data processing on the sensor, which reduces the energy consumed by the transmission of data. We conducted several experiments on a real datasets from healthy and epileptic patients to evaluate the performance and efficiency of our approach. We used a commercially available Micro Electro-Mechanical Systems (NEMS) and an Arduino Uno with wireless transmission to test our system and evaluate its performance. The prototype triggers an alarm upon the detection of life-threatening seizures and can be very effective in reducing SUDEP. The experimental results are encouraging, and demonstrate that our approach is able to achieve good detection accuracy with a low false alarm rate and low detection delay when compared with the state of the art PDF method.

In future work, we plan to deploy our developed system in the "epilepsies rares" department at the Necker-Enfant Malades Hospital in Paris, France, to cover more types of seizure. Among the challenges we would like to address as part of our future work are: miniaturization of the prototype system, addressing the difficulty in deploying the prototype and difficulty in fixing the electrode on the skin of disorderly and disruptive children, and optimizing of the algorithm to improve detection accuracy, especially in the presence of unreliable measurements from slightly detached electrodes.

More research is needed with larger datasets to further refine and optimize the performance of our detection system in order to detect the most common types of seizures among 40 known types. Currently, our approach is not able to detect without convulsions and with loss of muscle tone, such as gastaut seizures, where slightly impaired vision followed by adduction of the left eye only lasts for up to 10 seconds.

## REFERENCES

[1] P. Jallon, S. Bonnet, M. Antonakios, and R. Guillemaud, "Detection system of motor epileptic seizures through motion analysis with 3D accelerometers," in *Proc. 31st Annu. Int. Conf. IEEE Eng. Med. Biol. Soc.*, 2009, pp. 2466–2469.
[2] I. Conradsen, S. Beniczky, P. Wolf, J. Henriksen, T. Sams, and H. Sorensen, "Seizure onset detection based on a uni- or multi-modal intelligent seizure acquisition (UISA/MISA) system," in *Proc. Annu. Int. Conf. IEEE Eng. Med. Biol. Soc.*, 2010, pp. 3269–3272.
[3] L. Guo, D. Rivero, J. Dorado, J. R. Rabuñnal, and A. Pazos, "Automatic epileptic seizure detection in EEGs based on line length feature and artificial neural networks," *J. Neurosci. Methods*, vol. 191, no. 1, pp. 101–109, 2010.
[4] A. T. Tzallas, M. G. Tsipouras, D. G. Tsalikakis, E. C. Karvounis, L. Astrakas, S. Konitsiotis, and M. Tzaphlidou, *Automated Epileptic Seizure Detection Methods: A Review Study*. London, U.K: Intech, 2012, ch. 4, pp. 75–98.
[5] A. Van de Vel, M. Milosevic, B. Bonroy, K. Cuppens, L. Lagae, B. Vanrumste, S. Van Huffel, and B. Ceulemans, "Long-term accelerometry-triggered video monitoring and detection of tonic-clonic and clonic seizures in a home environment: Pilot study," *Epilepsy Behavior Case Rep.*, vol. 5, pp. 66–71, 2016.
[6] Embrace. [Online]. Available: https://www.empatica.com/, Last visited 2018, iNDIEGOGO Techology.
[7] O. Salem, Y. Rebhi, A. Boumaza, and A. Mehaoua, "Detection of nocturnal epileptic seizures using wireless 3-D accelerometer sensors," in *Proc. IEEE 16th Int. Conf. e-Health Netw. Appl. Serv.*, 2014, pp. 237–242.
[8] M. Schwartz, Ed., *EMG Methods for Evaluating Muscle and Nerve Function*. London, U.K.: InTech, 2012.
[9] I. Conradsen, S. Beniczky, P. Wolf, T. W. Kjaer, T. Sams, and H. B. D. Sorensen, "Automatic multi-modal intelligent seizure acquisition (MISA) system for detection of motor seizures from electromyographic data and motion data," *Comput. Methods Programs Biomed.*, vol. 107, no. 2, pp. 97–110, 2012.
[10] M. U. Saleheen, H. Alemzadeh, A. M. Cheriyan, Z. Kalbarczyk, and R. K. Iyer, "An efficient embedded hardware for high accuracy detection of epileptic seizures," in *Proc. 3rd Int. Conf. Biomed. Eng. Inform.*, 2010, pp. 1889–1896.
[11] Y. Zhang, B. Liu, X. Ji, and D. Huang, "Classification of EEG signals based on autoregressive model and wavelet packet decomposition," *Neural Process. Lett.*, vol. 45, no. 2, pp. 365–378, 2017.
[12] G. Chen, W. Xie, T. D. Bui, and A. Krzyżak, "Automatic epileptic seizure detection in eeg using nonsubsampled wavelet–fourier features," *J. Med. Biological Eng.*, vol. 37, no. 1, pp. 123–131, 2017.
[13] S. N. Baldassano, B. H. Brinkmann, H. Ung, T. Blevins, E. C. Conrad, K. Leyde, M. J. Cook, A. N. Khambhati, J. B. Wagenaar, G. A. Worrell, and B. Litt, "Crowdsourcing seizure detection: Algorithm development and validation on human implanted device recordings," *Brain*, vol. 140, no. 6, pp. 1680–1691, 2017.
[14] H. Polat and M. S. Ozerdem, "Epileptic seizure detection from EEG signals by using wavelet and Hilbert transform," in *Proc. 12th Int. Conf. Perspective Technol. Methods MEMS Des.*, 2016, pp. 66–69.
[15] C. Zhang, M. A. B. Altaf, and J. Yoo, "Design and implementation of an on-chip patient-specific closed-loop seizure onset and termination detection system," *IEEE J. Biomed. Health Informat.*, vol. 20, no. 4, pp. 996–1007, Jul. 2016.
[16] G. Becq, P. Kahane, L. Minotti, S. Bonnet, and R. Guillemaud, "Classification of epileptic motor manifestations and detection of tonic – clonic seizures with acceleration norm entropy," *IEEE Trans. Biomed. Eng.*, vol. 60, no. 8, pp. 2080–2088, Aug. 2013.
[17] U. Kramer, S. Kipervasser, A. Shlitner, and R. Kuzniecky, "A Novel Portable Seizure Detection Alarm System: Preliminary Results," *J. Clinical Neurophysiol*, vol. 28, no. 1, pp. 36–38, 2011.
[18] H. S. Joo, S.-H. Han, J. Lee, D. P. Jang, J. K. Kang, and J. Woo, "Spectral analysis of acceleration data for detection of generalized tonic-clonic seizures," *Sensors*, vol. 17, no. 3, 2017, Art. no. 481.
[19] M. Velez, R. S. Fisher, V. Bartlett, and S. Le, "Tracking generalized tonic-clonic seizures with a wrist accelerometer linked to an online database," *Seizure*, vol. 39, no. Supplement C, pp. 13–18, 2016.
[20] Epileply detect. [Online]. Available: http://www.epdetect.com/, Last visited 2018.
[21] Epi-care free. [Online]. Available: http://danishcare.dk/, Last visited 2018, danishCare Techology.
[22] W. J. van Elmpt, T. M. Nijsen, P. A. Griep, and J. B. Arends, "A model of heart rate changes to detect seizures in severe epilepsy," *Seizure*, vol. 15, no. 6, pp. 366–375, 2006.
[23] F. Massé, M. V. Bussel, A. Serteyn, J. Arends, and J. Penders, "Miniaturized wireless ECG monitor for real-time detection of epileptic seizures," *ACM Trans. Embed. Comput. Syst.*, vol. 12, no. 4, pp. 102:1–102:21, 2013.
[24] K. Fujiwara, M. Miyajima, T. Yamakawa, E. Abe, Y. Suzuki, Y. Sawada, M. Kano, T. Maehara, K. Ohta, T. Sasai-Sakuma, T. Sasano, M. Matsuura, and E. Matsushima, "Epileptic seizure prediction based on multivariate statistical process control of heart rate variability features," *IEEE Trans. Biomed. Eng.*, vol. 63, no. 6, pp. 1321–1332, Jun. 2016.
[25] Y.-L. Wang, S.-F. Liang, F.-Z. Shaw, A. Su, Y.-L. Chen, and S.-Y. Wu, "Use of accelerometers to detect motor states in a seizure of rats with temporal lobe epilepsy," in *Proc. IEEE Biomed. Circuits Syst. Conf.*, 2012, pp. 372–375.
[26] Y.-L. Wang, S.-F. Liang, F.-Z. Shaw, Y.-H. Huang, and S.-Y. Wu, "Detection of spontaneous temporal lobe epilepsy in rats by means of 1-axis accelerometor signal," in *Proc. 9th Int. Conf. Inf. Commun. Signal Process.*, 2013, pp. 1–5.
[27] T. M. Nijsen, R. M. Aarts, P. J. M. Cluitmans, and P. A. Griep, "Time-frequency analysis of accelerometry data for detection of myoclonic seizures," *IEEE Trans. Inf. Technol. Biomed.*, vol. 14, no. 5, pp. 1197–1203, Sep. 2010.
[28] G. T. Borujeny, M. Yazdi, A. Keshavarz-Haddad, and A. R. Borujeny, "Detection of epileptic seizure using wireless sensor networks," *J. Med. Signals Sensors*, vol. 3, no. 2, pp. 63–68, 2013.

[29] A. Dalton, S. Patel, A. Chowdhury, M. Welsh, T. Pang, S. Schachter, G. Olaighin, and P. Bonato, "Development of a body sensor network to detect motor patterns of epileptic seizures," *IEEE Trans. Biomed. Eng.*, vol. 59, no. 11, pp. 3204–3211, Nov. 2012.

[30] K. Cuppens, P. Karsmakers, A. Van de Vel, B. Bonroy, M. Milosevic, S. Luca, T. Croonenborghs, B. Ceulemans, L. Lagae, S. Van Huffel, and B. Vanrumste, "Accelerometry-based home monitoring for detection of nocturnal hypermotor seizures based on novelty detection," *IEEE J. Biomed. Health Inform.*, vol. 18, no. 3, pp. 1026–1033, May 2014.

[31] K. Cuppens, L. Lagae, B. Ceulemans, S. V. Huffel, and B. Vanrumste, "Detection of nocturnal frontal lobe seizures in pediatric patients by means of accelerometers: A first study," in *Proc. Int. Conf. IEEE Eng. Med. Biol. Soc.*, 2009, pp. 6608–6611.

[32] I. Cleland, B. Kikhia, C. Nugent, A. Boytsov, J. Hallberg, K. Synnes, S. McClean, and D. Finlay, "Optimal placement of accelerometers for the detection of everyday activities," *Sensors*, vol. 13, no. 7, pp. 9183–9200, 2013.

[33] G. Becq, S. Bonnet, L. Minotti, M. Antonakios, R. Guillemaud, and P. Kahane, "Collection and exploratory analysis of attitude sensor data in an epilepsy monitoring unit," in *Proc. 29th Annu. Int. Conf. IEEE Eng. Med. Biol. Soc.*, 2007, pp. 2775–2778.

[34] A. Tzallas, M. Tsipouras, and D. Fotiadis, "Epileptic seizure detection in EEGs using time-frequency analysis," *IEEE Trans. Inf. Technol. Biomed.*, vol. 13, no. 5, pp. 703–710, Sep. 2009.

[35] S. Larsen, I. Conradsen, S. Beniczky, and H. Sorensen, "Detection of tonic epileptic seizures based on surface electromyography," in *Proc. 36th Annu. Int. Conf. IEEE Eng. Med. Biol. Soc.*, 2014, pp. 942–945.

[36] I. Conradsen, S. Beniczky, P. Wolf, T. W. Kjaer, T. Sams, and H. B. Sorensen, "Automatic multi-modal intelligent seizure acquisition (MISA) system for detection of motor seizures from electromyographic data and motion data," *Comput. Methods Programs Biomed.*, vol. 107, no. 2, pp. 97–110, 2012.

[37] A. Harvey, *Forecasting with Unobserved Components Time Series Models*, vol. 1. Amsterdam, The Netherlands: Elsevier, 2006, ch. 7, pp. 327–412.

[38] P. Cisar, S. Bosnjak, and S. Maravic-Cisar, "EWMA algorithm in network practice," *Int. J. Comput. Commun. Control*, vol. 5, no. 2, pp. 160–170, 2010.

[39] Cooking-hacks, E-health Sensor Plateform. [Online]. Available: http://www.cooking-hacks.com/ehealth-sensors-complete-kit-biometric-medical-arduino-raspberry-pi, Last visited: Mar. 2018

[40] Thalmic Labs Inc., "Myo arm Band." [Online]. Available: https://support.getmyo.com/hc/en-us, Last visited 2018.

[41] M. Cognolato, M. Atzori, D. Faccio, C. Tiengo, F. Bassette, R. Gassert, and H. Muller, "Hand gesture classification in transradial amputees using the Myo armband classifier," in *Proc. 7th IEEE Int. Conf. Biomed. Robot. Biomechatronics*, 2018, pp. 156–161.

[42] G. D. Morais, L. C. Neves, A. A. Masiero, and M. C. F. Castro, "Application of Myo armband system to control a robot interface," in *Proc. Int. Joint Conf. Biomed. Eng. Syst. Technol.*, 2016, pp. 227–231.

[43] Shimmer Discovery in motion, *Shimmer ECG User Guide, Revision 1.12, Realtime Technologies Ltd*, 2017. [Online]. Available: https://www.shimmersensing.com/support/wireless-sensor-networks-documentation/category/12, Last visited: Aug. 2018.

[44] M. Nabian, A. Nouhi, Y. Yin, and S. Ostadabbas, "A biosignal-specific processing tool for machine learning and pattern recognition," in *Proc. IEEE Healthcare Innovations Point Care Technol.*, Nov. 2017, pp. 76–80.

[45] A. Van de Vel, K. Cuppens, B. Bonroy, M. Milosevic, S. V. Huffel, B. Vanrumste, L. Lagae, and B. Ceulemans, "Long-term home monitoring of hypermotor seizures by patient-worn accelerometers," *Epilepsy Behavior*, vol. 26, no. 1, pp. 118–25, 2013.

[46] E. McKenzie, A. S. P. Lim, E. C. W. Leung, A. Cole, A. Lam, A. Eloyan, D. Nirola, L. Tshering, R. Thibert, R. Z. Garcia, E. Bui, S. Deki, L. Lee, S. J. Clark, J. M. Cohen, J. Mantia, K. T. Brizzi, T. R. Sorets, S. Wahlster, and F. Mateen, "Validation of a smartphone-based EEG among people with epilepsy: A prospective study," *Sci. Rep.*, vol. 7, Apr. 2017, Art. no. 45567.

[47] Emotiv Inc., "Emotiv mobile EEG headset." [Online]. Available: https://www.emotiv.com, Last visited 2018.

[48] I. Conradsen, S. Beniczky, K. Hoppe, P. Wolf, and H. B. D. Sorensen, "Automated algorithm for generalized tonic-clonic epileptic seizure onset detection based on sEMG zero-crossing rate," *IEEE Trans. Biomed. Eng.*, vol. 59, no. 2, pp. 579–585, Feb. 2012.

**Osman Salem** received the MSc and PhD degrees in computer science from Paul Sabatier University, Toulouse, France, in 2002 and 2006, respectively, and the Habilitation À Diriger des recherches degree from the University of Paris Descartes, Paris, France, 2016. From 2006 to 2008, he was with the Department of Computer Science, Telecom Bretagne, Brest, France, as a postdoctoral research fellow. Since September 2008, he has been an associate professor with the University of Paris Descartes, Paris, France. His research interests include security and anomaly detection in medical wireless sensor networks.

**Khalid Alsubhi** received the BSc degree in computer science from King Abdulaziz University (KAU), in 2003, and the MMath and PhD degrees in computer science from the University of Waterloo, Canada, in 2009 and 2016, respectively. He is currently an assistant professor of computer science with KAU. His research interests include focused on network security and management, cloud computing, and security and privacy of healthcare applications.

**Ahmed Mehaoua** received the MSc and PhD degrees in computer science from the University of Paris, France, in 1993 and 1997, respectively. He is currently a full professor of computer communication with the Faculty of Mathematics and Computer Science, University of Paris Descartes, Paris, France. He is also the head of the Department of Multimedia Networking and Security, LIPADE, a governmental computer science research center in Paris, France. His research interests include wireless healthcare systems and networks and applications.

**Raouf Boutaba** received the MSc and PhD degrees in computer science from the University Pierre & Marie Curie, Paris, in 1990 and 1994, respectively. He is currently a professor of computer science and the associate dean research of the Faculty of Mathematics, University of Waterloo (Canada). His research interests include resource management in wired and wireless networks. He holds a university research chair in Waterloo and an INRIA international chair in France. He is the current editor in chief of the *IEEE Journal on Selected Areas in Communications*. He is a fellow of the IEEE, the Engineering Institute of Canada, and the Canadian Academy of Engineering.

▷ **For more information on this or any other computing topic, please visit our Digital Library at** www.computer.org/publications/dlib.